

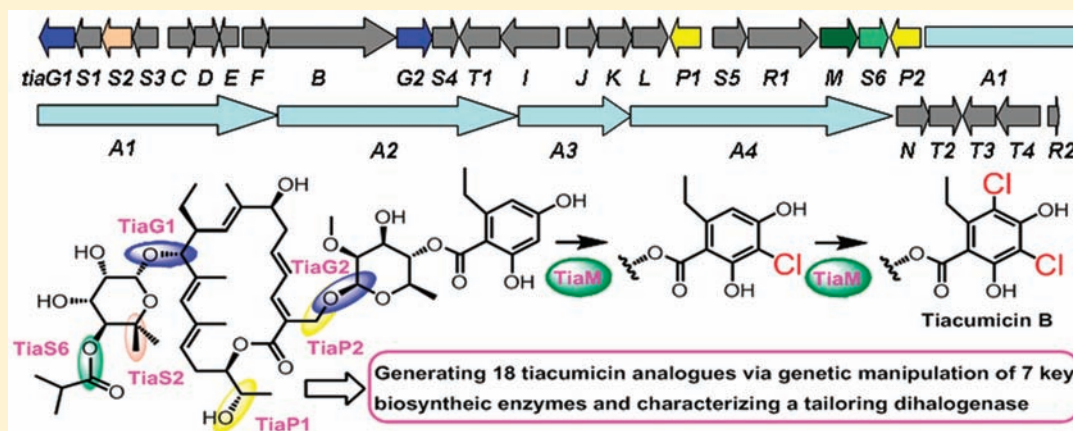
Characterization of Tiacumicin B Biosynthetic Gene Cluster Affording Diversified Tiacumicin Analogues and Revealing a Tailoring Dihalogenase

Yi Xiao,[†] Sumei Li,[†] Siwen Niu, Liang Ma, Guangtao Zhang, Haibo Zhang, Gaiyun Zhang, Jianhua Ju, and Changsheng Zhang*

CAS Key Laboratory of Marine Bio-resources Sustainable Utilization, RNAM Center for Marine Microbiology, Guangdong Key Laboratory of Marine Materia Medica, South China Sea Institute of Oceanology, Chinese Academy of Sciences, 164 West Xingang Road, Guangzhou 510301, P.R. China

S Supporting Information

ABSTRACT:



The RNA polymerase inhibitor tiacumicin B is currently undergoing phase III clinical trial for treatment of *Clostridium difficile* associated diarrhea with great promise. To understand the biosynthetic logic and to lay a foundation for generating structural analogues via pathway engineering, the tiacumicin B biosynthetic gene cluster was identified and characterized from the producer *Dactylosporangium aurantiacum* subsp. *hamdenensis* NRRL 18085. Sequence analysis of a 110 633 bp DNA region revealed the presence of 50 open reading frames (orfs). Functional investigations of 11 orfs by *in vivo* inactivation experiments, preliminarily outlined the boundaries of the *tia*-gene cluster and suggested that 31 orfs were putatively involved in tiacumicin B biosynthesis. Functions of a halogenase (TiaM), two glycosyltransferases (TiaG1 and TiaG2), a sugar C-methyltransferase (TiaS2), an acyltransferase (TiaS6), and two cytochrome P450s (TiaP1 and TiaP2) were elucidated by isolation and structural characterization of the metabolites from the corresponding gene-inactivation mutants. Accumulation of 18 tiacumicin B analogues from 7 mutants not only provided experimental evidence to confirm the proposed functions of individual biosynthetic enzymes, but also set an example of accessing microbial natural product diversity via genetic approach. More importantly, biochemical characterization of the FAD-dependent halogenase TiaM reveals a sequentially acting dihalogenation step tailoring tiacumicin B biosynthesis.

INTRODUCTION

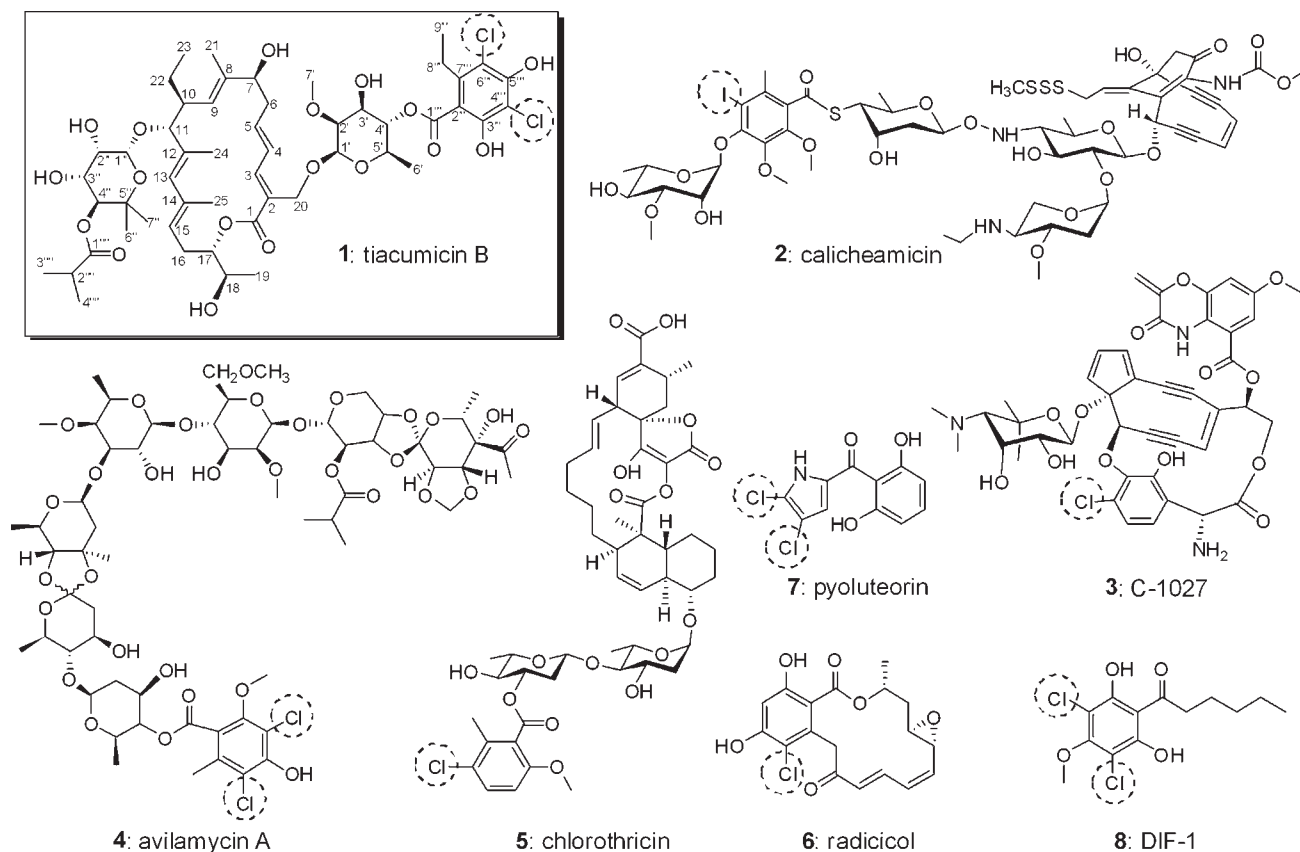
Tiacumicin B (**1**, Chart 1), also known as lipiarmycin A3, PAR-101, OPT-80, Difimicin and Fidaxomicin,¹ is produced by *Dactylosporangium aurantiacum* subsp. *hamdenensis* NRRL 18085,² *Actinoplanes deccanensis* ATCC 21983,^{3,4} *Micromonospora echinospora* subsp. *armeniaca*,⁵ and *Catellatospora* sp. Bp3323-81.⁶ Tiacumicin B (**1**) is a broad-spectrum antibiotic against various Gram-positive pathogenic bacteria, especially diarrhea-associated *Clostridium difficile*, with low minimal inhibitory concentration

(MIC) values.^{7–10} Recently, tiacumicin B was demonstrated to be effective against multidrug-resistant *Mycobacterium tuberculosis* strains with no cross-resistance to rifampicin,⁶ and was also shown to exhibit good anticancer activities.¹¹ Currently, tiacumicin B is undergoing phase III clinical trials, developed by Optimer Pharmaceuticals, Inc., for the treatment of *C. difficile* infection (CDI).

Received: October 20, 2010

Published: December 27, 2010

Chart 1. Chemical Structures for Tiacumicin B (1), Calicheamicin γ_1^1 (2), C-1027 (3), Avilamycin A (4), Chlorothricin (5), Radicol (6), Pyoluteorin (7), and DIF (8)^a



^a Halogens are highlighted by dashed circles.

Tiacumicin B is shown to be statistically superior to vancomycin, the only FDA approved product for CDI, in better global cure rates and fewer relapses (<http://www.optimerpharma.com>). Additionally, tiacumicin B exhibits no toxicities in animal studies,¹² making it a promising drug candidate. However, the mechanism of tiacumicin action is not well understood. Tiacumicin B is found as a bacterial RNA polymerase inhibitor and inhibits the holoenzyme better than the core enzyme.^{3,13} Recent genetic and biochemical studies reveal that tiacumicin B blocks the early step of open-promoter-complex formation, suggesting a new mechanism of transcription inhibitor action.¹⁴

The chemical structure of tiacumicin B (1) was elucidated by extensive spectral analyses and was finally confirmed by X-ray crystallographic studies.^{2,4,15–17} Tiacumicin B belongs to a family of novel 18-membered macrocyclic glycosides and contains an unsaturated macrolide core scaffold, two modified D-rhamnose residues, and a dichlorinated homo-orsellinic acid moiety (Figure 1). Tiacumicin B is a member of halogenated natural products which comprise diverse structures (Chart 1, 1–8), exemplified by enediynes (calicheamicin γ_1^1 , 2, and C-1027, 3),^{18,19} orthosomycins (avilamycin A, 4),²⁰ macrolides (chlorothricin, 5, and radicol, 6),^{21–23} hybrid polyketide-nonribosomal peptides (pyoluteorin, 7),²⁴ and small hormone molecules (DIF-1, 8),²⁵ displaying a wide range of biological activities including antibacterial, antitumor, and quorum sensing properties. Recently, a variety of nature's strategies for biohalogenation have been demonstrated both biochemically and structurally.^{26–28}

For example, SgcC3 and PltA were shown to catalyze chlorinations on substrates tethered with discrete carrier proteins in C-1027 (3) and pyoluteorin (7) biosynthesis,^{19,24} respectively. ChlA-catalyzed dichlorinations on a free small molecule were demonstrated to be a tailoring strategy for DIF-1 (8) biosynthesis.²⁵ Structurally, 1, 2, 4, and 5 contain a similar halogenated aromatic moiety of polyketide origin as 8; however, the halogenation strategies for these molecules remain uncharacterized.

The structure–activity relationship studies reveal that tiacumicin B with an *R*-hydroxyl group at C-18 is more potent than its *S*-congener for antibacterial activity.¹⁶ Up to date, most 1 analogues were isolated from the producing strains by varying fermentation conditions;^{16,17,29} chemical efforts to diversify 1 were limited to make 1 benzylidene acetal derivatives for anticancer evaluations.¹¹ The unavailability of 1 genetic locus impeded the alternative to access 1 structural diversity via pathway engineering. To this end, herein we report the cloning and characterization of the intact 1 biosynthetic gene cluster from *D. aurantiacum* NRRL 18085. The sequencing of the entire *tia* gene cluster allows the assignment of functions to deduced gene products, and paves the way to genetic and biochemical characterization of the 1 biosynthetic pathway. Structural elucidation of eighteen 1 analogues accumulated from 7 key *tia* gene-inactivation mutants not only provides experimental evidence to confirm the proposed functions of individual biosynthetic enzymes, but also sets an example of accessing microbial natural product diversity via genetic approach. More importantly, the biochemical characterization of

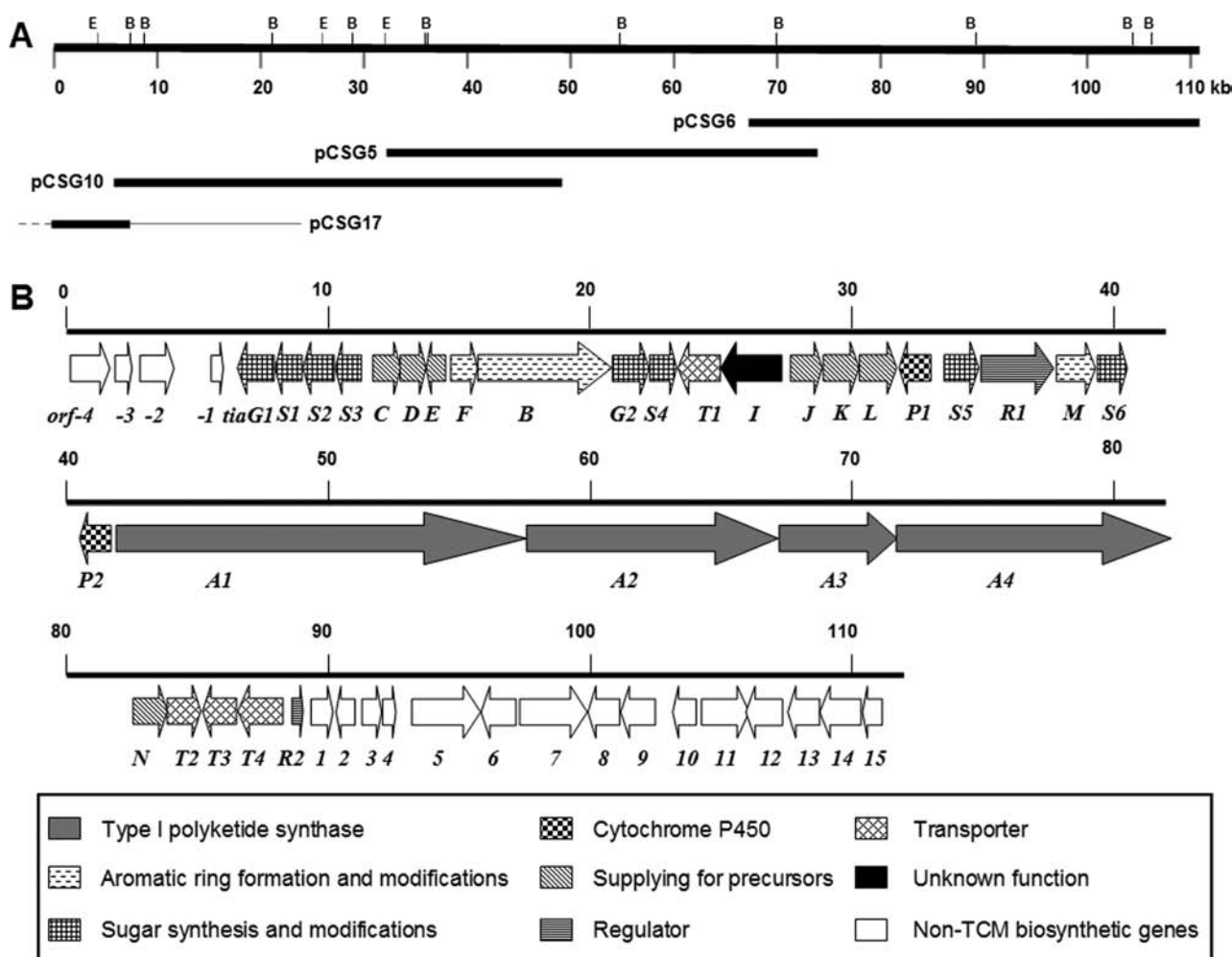


Figure 1. The restriction map of sequenced DNA region on *D. aurantiacum* chromosome and genetic organization of the *tia* gene cluster. (A) Restriction map of a sequenced 110.6 kb contiguous DNA region. Solid black bars show the sequenced regions of selected positive cosmids. E, *EcoRI*; B, *BglIII*. (B) Genetic organization of the *tia* gene cluster. Proposed functions of individual open reading frames (*orfs*) are labeled and summarized in Table 1.

a FAD-dependent halogenase TiaM reveals a sequentially acting dihalogenation step tailoring I biosynthesis. TiaM represents the first characterized tailoring halogenase of prokaryotic origin.

EXPERIMENTAL SECTION

Bacterial Strains, Plasmids, and Reagents. Strains and plasmids used and generated in this study are listed in Table S1. *D. aurantiacum* subsp. *hamdenensis* NRRL 18085 was obtained from Agricultural Research Service (ARS) Culture Collection (NRRL). Chemicals and reagents for biochemical and molecular biology were purchased from standard commercial sources.

DNA Isolation, Manipulation, and Sequencing. DNA isolation and manipulations in *Escherichia coli* and *Actinomyces* were performed according to standard procedures.^{30,31} PCR amplifications were carried out on an Authorized Thermal Cycler (Eppendorf AG). Primers were synthesized in Sangon Biotech (Shanghai) Co. Ltd. DNA sequencing was performed at the Invitrogen Biotech Co., Ltd. (Guangzhou), the Major Biotech Co., Ltd. (Shanghai), and Chinese National Genome Center (Shanghai).

Genomic Library Construction and Screening. A genomic library of *D. aurantiacum* NRRL 18085 was constructed in SuperCos1 by using the Gigapack III Gold Packaging Extract system according to the

manufacturer's instructions (Stratagene). A 0.55 kb halo-probe for halogenase was amplified by adopting previously reported primers 5'-TTCCSCGSTACCCASATCGGSGAG-3' (forward) and 5'-GSGGG-ATSWMCCAGWACCASCC-3' (reverse),³² and confirmed by cloning, sequencing, and blasting. A ~0.7 kb DNA fragment targeting modular type I polyketide synthases was amplified using the primers 5'-CTW-CGTSGAGGCSCAYGGCACSGG-3' (forward) and 5'-CCRTGMCC-SGAGAASACCCASAC-3' (reverse). DNA sequencing revealed two different types of sequences, designated as PKS probe-I (in pCSG1104) and PKS probe-II (in pCSG1105), respectively (Table S1). These 3 probes (halo-probe, PKS probes I and II) were used to screen against approximately 2000 colonies by colony hybridization using DIG High Prime DNA Labeling and Detection Starter Kit I (Roche), and resultant positive clones were further confirmed by PCR. Overlaps between positive clones were determined by restriction analyses. Detailed procedures were described in the Supporting Information.

Sequence Analysis. The DNA sequence of the *tia* gene cluster has been deposited into GenBank under the accession number HQ011923. The *orfs* were determined by using the FramePlot 4.0beta program (<http://nocardia.nih.gov/jp/fp4/>). Protein sequences were compared with BLAST programs (<http://blast.ncbi.nlm.nih.gov/Blast.cgi>). Domain organization and substrate specificities for PKSs were predicted by PKS/NRPS analysis program (<http://www.nii.res.in/searchall.html>).

Gene Inactivation Experiments. The lambda-RED-mediated gene replacements were performed as standard procedures.^{33,34} The gene inactivation experiments in *D. aurantiacum* NRRL 18085 were carried out using a recently developed genetic manipulation system.³⁵ Detailed procedures for individual gene inactivation were described in Supporting Information (Tables S1 and S2, Figure S2).

Production, Isolation, and Structural Elucidation of Tia-cumicin B and Its Analogues. The wild type strain *D. aurantiacum* NRRL 18085 and the mutants were cultured in YMS (Yeast extract 0.4%, malt extract 1%, soluble starch 0.4%, $\text{CoCl}_2 \cdot 6\text{H}_2\text{O}$ 5 mg/L, pH 7.2–7.4) or ISP2 medium (Yeast extract 0.4%, malt extract 1%, glucose 0.4%, pH 7.2) for 3–5 days. The 5% inoculums were seeded in 200 mL of production medium (Fish powder 1%, glucose 2%, yeast extract 0.25%, casamino acid 0.25%, CaCO_3 0.3%, K_2HPO_4 0.05%, $\text{MgSO}_4 \cdot 7\text{H}_2\text{O}$ 0.05%, KCl 0.03%, XAD-16 resin 4%, pH 7.0) in 1 L flask and then shaken at 250 rpm and 30 °C for 5–10 days.³⁶ The production of **1** and its analogues was monitored via HPLC analysis on a Varian Star Workstation. HPLC was carried out using a reversed phase column Luna C18, 5 μm , 150 \times 4.6 mm (Phenomenex) with UV detection at 254 nm under the following program: solvent system (solvent A, 10% acetonitrile in water supplementing with 0.08% trifluoroacetic acid (TFA); solvent B, 90% acetonitrile in water); 5% B to 100% B (linear gradient, 0–20 min), 100% B (20–21 min), 100% B to 5%B (21–22 min), 5% B (22–30 min); flow rate at 1 mL/min. For isolation of the product from the *tiaM* mutant TCMS0, the XAD-16 resin was separated by sieving from approximately 6 L fermentation broths and then eluted with ethanol. Ethanol was evaporated and the oily residues were extracted 5 times with ethyl acetate to afford crude extracts after evaporation. The crude extracts were subjected to silica gel column chromatography (300–400 mesh, 150 g) and eluted with $\text{CHCl}_3/\text{CH}_3\text{OH}$ (100:0 to 0:100) to give 4 fractions (Fr.1 to Fr.4). Each fraction was monitored by HPLC. The Fr.3 containing the desired product was subjected to Sephadex LH-20 and eluted with $\text{CHCl}_3/\text{CH}_3\text{OH}$ (1:1). Desired fractions were collected and further purified by semipreparative C18 reverse phase HPLC (YMC*GEL ODS-A, 12 nm S-50 μm , 30 \times 2.5 cm i.d.), eluting with a linear gradient ($\text{CH}_3\text{CN}/\text{H}_2\text{O}$ 5–72%, 120 min), to afford 210.0 mg of **9**. Detailed procedures for the isolation of compounds **10**–**26** were described in Supporting Information, supplemental methods. ¹H- and ¹³C NMR and 2D NMR spectra were recorded on a Bruker AV-500 MHz NMR spectrometer with tetramethylsilane (TMS) as internal standard. Mass spectral data were obtained on a quadrupole-time-of-flight mass spectrometry (Waters) for the HRFABMS (High Resolution Fast Atom Bombardment Mass Spectrometry). The optical rotation was recorded on a 341 polarimeter from Perkin-Elmer. Spectral data of structural elucidation for compounds **9**–**26** were summarized in Supporting Information (Tables S3 and S4, Figures S3–S19).

Heterologous Production and Purification of TiaM and SsuE. The *tiaM* gene was PCR-amplified from genomic DNA of *D. aurantiacum* NRRL 18085 using the following primer pair: 5'-GGAC-CATATGCCAAAGGTAATCGTC-3' (forward, *NdeI*) and 5'-CAT-GAATTCCTCCTCAAG GTGGGGA-3' (reverse, *EcoRI*) with high fidelity DNA polymerase Pyrobest (Takara). The FAD-reductase gene *ssuE* was amplified from genomic DNA of *E. coli* BL21(DE3) with primers 5'-GGAGAGCATATGCGTGTATCACCCTG-3' (forward, *NdeI*) and 5'-CAGGAATTCTTACGCATG GGCATTAC-3' (reverse, *EcoRI*). Both PCR products were digested with *NdeI/EcoRI* and inserted into pET28a, to give the expression plasmids pCSG99 (for *tiaM*) and pCSG117 (for *ssuE*) after sequence confirmation (Table S1), respectively. Strains *E. coli* BL21(DE3) carrying pCSG99 or pCSG117 were grown in LB medium at 37 °C to an A_{600} of around 0.7 and the expression of TiaM or SsuE was then induced by the addition of 0.1 mM of isopropyl- β -D-thiogalactopyranoside (IPTG) for 4–5 h at 20–25 °C. *N*-(His)₆-tagged TiaM and SsuE were purified via affinity chromatography. Cells were disrupted by sonification on ice in the binding buffer (300 mM NaCl, 50 mM sodium phosphate buffer, 10 mM imidazole, pH 7.4).

The cellular lysates were centrifuged at 13 500 *g* for 0.5 h. SsuE was further purified by nickel-nitrilotriacetic acid (Ni^{2+} -NTA) agarose (Invitrogen) according to the manufacturer's protocols. The purification of TiaM was achieved by loading supernatants onto a HisTrap HT column (1 mL, GE Healthcare) on a Fast protein liquid chromatography (FPLC, GE Healthcare) and eluting with a linear gradient of 10–500 mM imidazole in 50 mM sodium phosphate buffer (pH 7.4). The purified protein was desalted through PD-10 column (GE Healthcare) and stored in 50 mM phosphate buffer (pH 7.4) containing 1 mM dithiothreitol (DTT) and 20% glycerol at –80 °C until use.

Enzyme Assays. A standard TiaM assay mixtures contained 26 μM **9**, 0.1 mM FAD, 4 mM NADH, 100 mM NaCl, 2.9 μM TiaM, and 0.22 μM SsuE in 50 mM phosphate buffer (pH 7.4) in a total volume of 100 μL . The reaction was performed at 30 °C for 2 h. Then assay mixtures were extracted with 3 vol of ethyl acetate. After removing ethyl acetate by vacuum evaporation, the residues were dissolved in methanol and subjected to HPLC analysis. To isolate the enzymatic products, reactions were scaled up to 450 mL using TiaM crude extracts instead of purified proteins and the incubation time was prolonged to 4 h. Finally, 1.2 mg of **29** was purified from the reaction mixture as a white solid. Spectral data of structural elucidation for compound **29** were summarized in Supporting Information (Tables S3 and S4, Figure S20).

RESULTS

Cloning and Sequencing of the Tiacumicin B Gene Cluster from *D. aurantiacum* NRRL 18085. We set out to probe the **1** biosynthetic gene cluster by PCR with degenerate primers targeting type I polyketide synthase (PKS) and halogenase genes. We retrieved a halogenase probe (halo-probe) and two PKS probes I and II (see Experimental Section for details) by PCR. Subsequently, the digoxigenin-(DIG)-labeled halo-probe and PKS-probes I and II were utilized to screen approximately 2000 clones of a SuperCos1-based genomic library of *D. aurantiacum* NRRL 18085. Using the PKS-probes I and II, the same set of 16 positive cosmids (pCSG1–pCSG16) was isolated, of which 8 cosmids were also positive with the halo-probe. Next, the target PKS I allele was inactivated by a genetic system previously developed for the producer *D. aurantiacum* NRRL 18085.³⁵ The resulting mutant lost the ability to produce **1**, suggesting its involvement in **1** biosynthesis. Finally, restriction analyses of the 16 positive cosmids revealed that they overlapped in a DNA region of approximately 105 kb (Figure S1). End-sequencing of the left-hand side of pCSG10 suggests the need for further extension to cover the entire **1** gene cluster. Therefore, additional chromosomal walking was performed from the left end of pCSG10 by PCR (Figure 1), resulting in the identification of two positive clones, namely, pCSG17 and pCSG18 (Figure S1). Three overlapping cosmids, pCSG5, pCSG6, and pCSG10, were entirely sequenced by a shotgun approach. For covering the entire *tia*-gene cluster, approximately 5 kb DNA fragment in pCSG17, upstream of the left-end of pCSG10 (Figure S1), was further analyzed by subcloning and sequencing. Finally, a total of 110 633 bp contiguous sequence was determined to encompass the complete *tia*-gene cluster. Bioinformatic analysis of the sequenced region reveals an overall high GC content (71.2%) and 50 *orfs* (Figure 1). The deduced functions of individual *orfs* are summarized in Table 1, assigned by comparison with known proteins in database.

Preliminary Determination of the *tia*-Gene Cluster Boundaries. Both genes *orf*(–1) and *orf*(–2) encode putative transposases, and the *orf*(–3) encodes a hypothetical protein (Table 1), showing no relevance to **1** biosynthesis. We inactivated the

Table 1. Deduced orf Functions in the *tia* Biosynthetic Gene Cluster

Gene	size ^a	protein homologue ^b	proposed function
<i>orf(-4)</i>	372	Sros_9042 (YP_003344414, 58/41)	Hypothetical protein
<i>orf(-3)</i>	212	BCE_2619 (NP_978925, 47/28)	Hypothetical protein
<i>orf(-2)</i>	430	TTE1786 (NP_623376, 45/25)	Transposase
<i>orf(-1)</i>	154	StreC_010100037728 (ZP_05511481,75/60)	Transposase
<i>tiaG1</i>	465	FscMI (AAQ82555, 53/38)	Glycosyltransferase
<i>tiaS1</i>	338	Gmd (ABM72507, 76/58)	GDP-D-mannose 4,6-dehydratase
<i>tiaS2</i>	402	SnoG (AAF01816, 54/37)	C-methyltransferase
<i>tiaS3</i>	332	NysDIII (AAF71765, 75/59)	GDP-D-mannose 4,6-dehydratase
<i>tiaC</i>	353	BkdF (AAB03377, 65/51)	Branched-chain alpha-keto acid dehydrogenase E1-alpha subunit
<i>tiaD</i>	325	BkdB (AAA66073, 68/53)	Branched-chain alpha-keto acid dehydrogenase E1-beta subunit
<i>tiaE</i>	248	NysE (AAF71777, 72/61)	Type II thioesterase
<i>tiaF</i>	343	ChlB3 (AAZ77676, 74/58)	Ketoacyl-ACP synthase
<i>tiaB</i>	1709	ChlB1 (AAZ77673, 61/49)	Iterative type I PKS
<i>tiaG2</i>	473	PimK (CAC20918,58/42)	Glycosyltransferase
<i>tiaS4</i>	343	AmphDIII (AAK73500,83/71)	GDP-D-mannose 4,6-dehydratase
<i>tiaT1</i>	541	CalT1 (AAM94765, 70/52)	Membrane transport protein
<i>tiaI</i>	783	Amir_1311 (YP_003099109, 69/56)	Superfamily I DNA and RNA helicase
<i>tiaJ</i>	410	FraEuI1cDRAFT_4757 (EFA60052, 60/50)	3-hydroxybutyryl-CoA dehydrogenase
<i>tiaK</i>	454	RimJ (AAR16523, 83/74)	Crotonyl-CoA carboxylase/reductase
<i>tiaL</i>	476	Strop_2764 (ABP55206, 77/66)	Propionyl-CoA carboxylase
<i>tiaP1</i>	392	LnmA (AAN85514, 52/39)	Cytochrome P450 hydroxylase
<i>tiaS5</i>	441	StfMIII (CAJ42340, 55/39)	Sugar O-methyltransferase
<i>tiaR1</i>	923	Orf3 (AAZ94383, 54/40)	LuxR class regulator
<i>tiaM</i>	494	CrpH (ABM21576, 60/40)	Halogenase
<i>tiaS6</i>	379	TcaM (ACB37733, 59/43)	O-acyltransferase
<i>tiaP2</i>	399	Sros_6255 (ACZ88980, 71/60)	Cytochrome P450
<i>tiaA1</i>	5229	PteA1 (BAB69303, 59/47)	Modular polyketide synthase
<i>tiaA2</i>	3205	TamAII (ADC79638, 62/49)	Modular polyketide synthase
<i>tiaA3</i>	1502	MerA (ABC87509, 64/52)	Modular polyketide synthase
<i>tiaA4</i>	3461	VinP4 (BAD08360, 58/47)	Modular polyketide synthase
<i>tiaN</i>	399	DpgC (AAM80546, 49/35)	Enoyl-CoA hydratase/isomerase
<i>tiaT2</i>	428	GntQ (AAR98563, 70/53)	Na/H membrane antiporter
<i>tiaT3</i>	437	Tpau_3325 (ADG79910, 70/58)	ABC transporter related protein
<i>tiaT4</i>	584	CYA_1065 (ABC99260, 68/53)	NitT/TauT family ABC transporter
<i>tiaR2</i>	137	MT0849 (AAK45091, 56/42)	ArsR family transcriptional regulator
<i>orf1</i>	282	GOX1538 (AAW61280, 79/60)	Short chain dehydrogenase
<i>orf2</i>	241	GY4MC1DRAFT_2771 (EET69906, 63/49)	Cystathionine gamma-synthase
<i>orf3</i>	249	ORF114 (BAC76572, 78/65)	Glucose dehydrogenase
<i>orf4</i>	166	MSMEG_6824 (ABK75393, 70/60)	MarR-family protein regulatory protein
<i>orf5</i>	870	Caci_3613 (YP_003114357, 43/32)	LuxR family transcriptional regulator
<i>orf6</i>	447	STIAU_3934 (ZP_01460872, 54/41)	Hypothetical protein
<i>orf7</i>	851	MSMEG_2120 (YP_886478, 40/28)	TPR repeat-containing protein
<i>orf8</i>	405	Gll4265 (NP_927211, 52/35)	Hypothetical protein
<i>orf9</i>	439	Sros_2893 (YP_003338592, 59/46)	Alkaline phosphatase
<i>orf10</i>	296	LBPG_01476 (ZP_04673774, 62/46)	3-hydroxyisobutyrate dehydrogenase
<i>orf11</i>	604	TcurDRAFT_17220 (ZP_04030703, 40/29)	Hypothetical protein
<i>orf12</i>	464	SACE_6077 (YP_001108175, 79/65)	Bicyclomycin resistance protein TcaB
<i>orf13</i>	405	RHOER0001_0914 (ZP_04387995, 57/43)	D-amino acid deaminase
<i>orf14</i>	531	NdaD (CAB49065, 53/36)	Probable D-aminoacylase
<i>orf15</i>	254	Bcav_1462 (YP_002881482, 57/41)	IclR family transcriptional regulator

^a Sizes are in amino acids. ^b Accession numbers and percentages of similarity/identity are given in parentheses.

gene *orf(-1)* via replacement of the *aac(3)IV* gene cassette to obtain a mutant TCM58 (Figure S2A). HPLC-MS analysis

revealed that TCM58 produced a single major product with the same retention time (17.7 min) and the same molecular weight

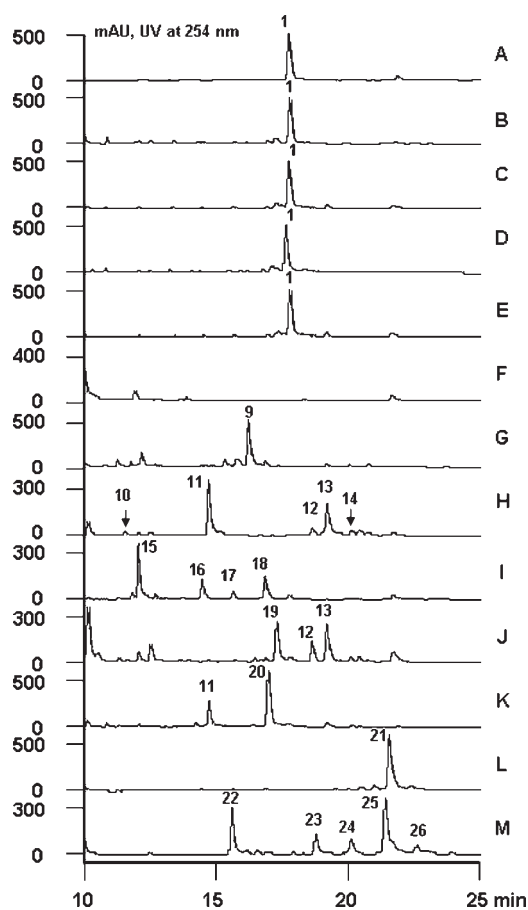
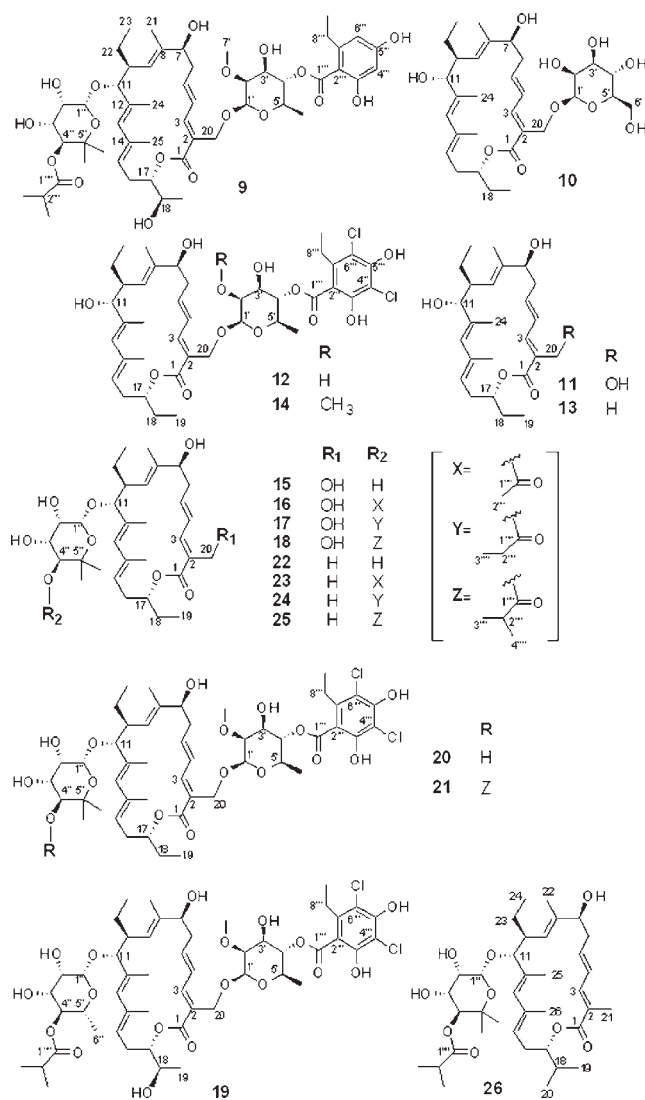


Figure 2. HPLC analyses of metabolite profile of *tia*-gene-inactivated mutants. (A) Tiacumicin B standard; (B) wild-type *D. aurantiacum* NRRL 18085; (C) TCM58 ($\Delta orf(-1)$); (D) TCM73 ($\Delta orf1$); (E) TCM72 ($\Delta tiaR2$); (F) TCM77 ($\Delta tiaA1$); (G) TCM50 ($\Delta tiaM$); (H) TCM57 ($\Delta tiaG1$); (I) TCM64 ($\Delta tiaG2$); (J) TCM55 ($\Delta tiaS2$); (K) TCM53 ($\Delta tiaS6$); (L) TCM69 ($\Delta tiaP1$); (M) TCM54 ($\Delta tiaP2$). Newly generated compounds are indicated and their structures are shown in Chart 2.

(m/z 1079.4, $[M + Na]^+$) as that produced by the wild-type strain and the **1** standard (Figure 2A–C). The production level was comparable to the wild-type strain, suggesting that *orf(-1)* is beyond the *tia*-gene cluster. In contrast, the inactivation of a putative glycosyltransferase (GT)-encoding gene *tiaG1* (Figure S2B), immediately downstream of *orf(-1)*, led to the abolishment of **1** production and the accumulation of new products (Figure 2H), confirming that *tiaG1* plays an essential role in **1** biosynthesis. The downstream boundary of the *tia*-gene cluster is intriguing. From the bioinformatic analysis, the deduced products of *orfs1–15* exhibit no significant functions putatively related to **1** biosynthesis (Table 1). The inactivation of *orf1* (Figure S2C), encoding a putative short chain dehydrogenase, led to the mutant TCM73 exhibiting no effects on **1** production (Figure 2D), clearly excluding its role in **1** biosynthesis. Subsequently, the gene *tiaR2*, encoding a putative ArsR family transcriptional regulator, immediately next to *orf1*, was also inactivated (Figure S2D). The resulting mutant TCM72 still produced **1** (Figure 2E), however, at a slightly enhanced level, arguably indicating that *tiaR2* is a putative negative regulator. These experimental results, together with the functional assignment of individual *orfs* by bioinformatic analyses, suggest that the *tia* gene cluster presumably contains 31

Chart 2. Chemical Structures of Compounds Generated by *tia*-Gene-Inactivated Mutants



orfs flanked by *tiaG1* and *tiaR2*, and spans a DNA region of approximately 83 kb (Figure 1, Table 1).

Biosynthesis of the Tiacumicin Aglycone, Tiacumicinone.

Four genes, *tiaA1–tiaA4*, encoding the multifunctional type I modular PKSs, are transcribed in the same direction and arranged collinearly with their predicted functional domains for loading, chain elongation, and modification, as outlined in Figure 3A. The *tia* type I PKSs consist of a loading module and 8 extending modules, comprising 40 predicted functional domains. The loading module contains the acyltransferase (AT_L) and the acyl carrier protein (ACP_L) domains. Propionyl-CoA is proposed to be a starter unit initiating the PKS assembly in **1** biosynthesis (Figure 3A), similar to 6-deoxyerythronolide B synthase (DEBS) in erythromycin biosynthesis.^{37,38} Sequence analysis of AT domains in extending modules reveals three distinct motifs believed to be directly involved in substrate selectivity: “Q...GHSIGE...HAFH” in modules 1, 6 and 7, specific for malonyl-CoA; “Q...GHSQGE...YASH” in modules 2, 3, 5 and 8, specific for (2S)-methylmalonyl-CoA; and “Q...GSSQGE...VASH” in the module 4, specific for (2S)-ethylmalonyl-CoA.³⁹ The substrate specificities of these AT domains match perfectly to the extender units predicted in the

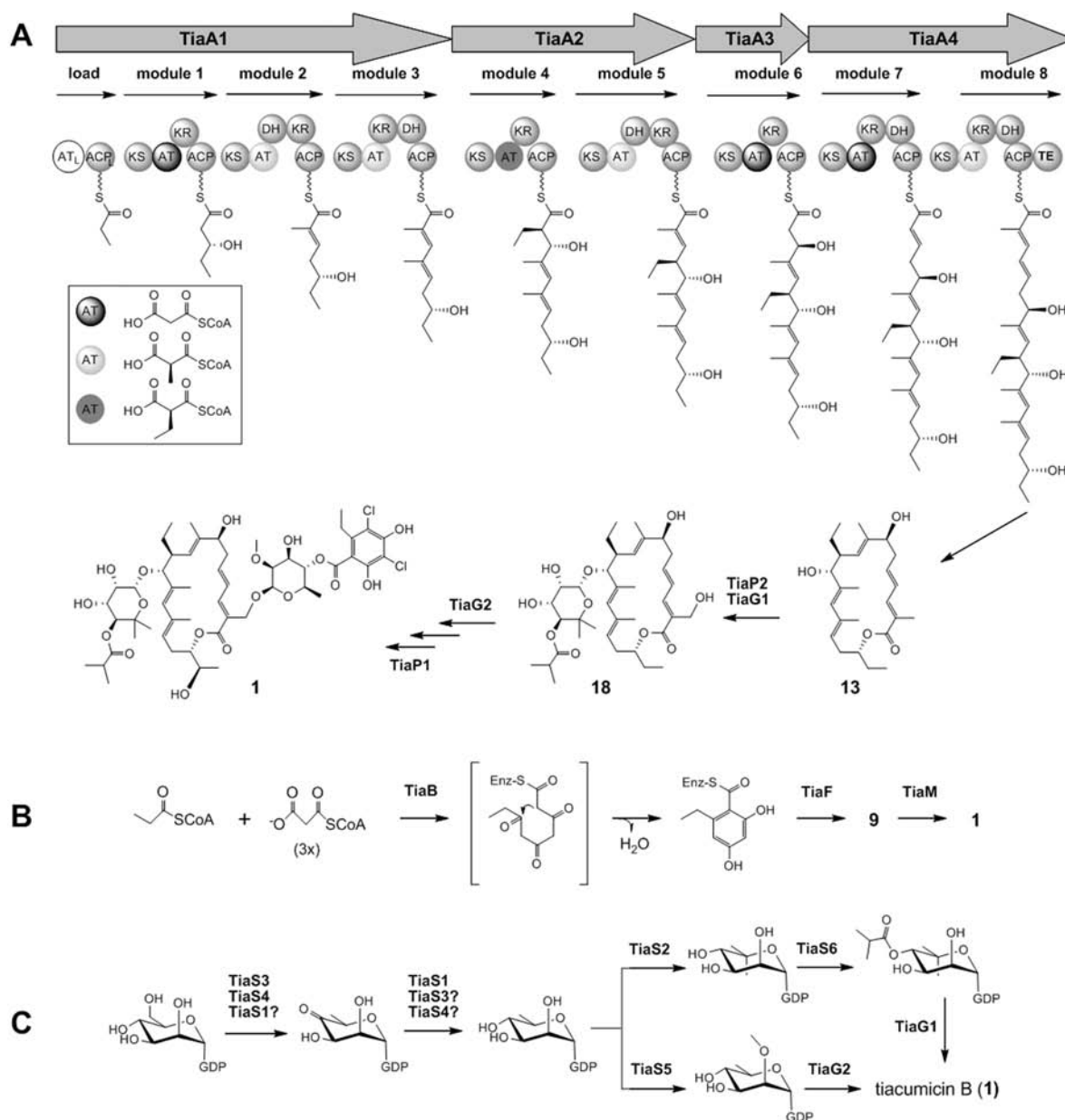


Figure 3. Proposed biosynthetic pathway for tiacumicin B. (A) A model for PKS-directed skeleton assembly and tailoring modifications; (B) pathway for the homo-orsellinic acid moiety; (C) pathway for biosynthesis and modifications of deoxysugar moieties.

PKS assembly line of **1** biosynthesis (Figure 3A). In our *in vivo* experiments, the *tiaA1*-inactivation mutant TCM77 lost the ability to produce **1** (Figure 2F, Figure S2E). Consequently, we propose that TiaA1–A4, in a mechanistic analogy to a typical noniterative type I PKS, catalyze the formation of the 18-membered macrocyclic aglycone, tiacumicinone (**13**, Figure 3A).

Biosynthesis and Modification of the Homo-Orsellinic Acid Moiety. The deduced product of *tiaB* contains characteristic type I PKS domains and is supposed to be responsible for the biosynthesis of the aromatic moiety (homo-orsellinic acid) in **1**. Bioinformatic analysis shows that TiaB carries PKS domains for ketosynthase (KS), AT, dehydratase (DH), keto reductase (KR) and ACP, and displays the highest sequence similarity to ChlB1, a 6-methyl-salicylic acid synthase.^{21,40} However, the DH domain lacks the conserved motif (HxxxGxxxxP) for activity,⁴¹ and the

characteristic Rossmann-fold of NADP(H) binding motif is not identified in the KR domain, implying that both KR and DH domains in TiaB are inactive. Indeed, formation of the homo-orsellinic acid moiety in **1** does not require functional KR and DH domains (Figure 3B). However, distinct from orsellinic acid synthases CalO5 and AviM,^{18,20} TiaB may utilize an unusual propionyl-CoA but not acetyl-CoA as a starter unit, leading to the formation of homo-orsellinic acid moiety. Immediately upstream of *tiaB*, there lies the *tiaF* gene. TiaF shares high sequence similarities to acyltransferases, such as ChlB3 (58% identity) and ChlB6 (34% identity) for chlorothricin (**5**),^{21,42} CalO4 (55% identity) for calicheamicin γ_1^1 (**2**),¹⁸ and AviN (51% identity) for avilamycin A (**4**),²⁰ which are all putatively responsible for incorporation of an aromatic moiety into the corresponding secondary metabolites (Chart 1). Therefore, we suppose that TiaF likely

transferred the homo-orsellinic acid moiety to the 2-*O*-methyl-*D*-rhamnose residue. A single FADH₂-dependent halogenase-encoding gene, *tiaM*, is identified in the *tia* gene cluster. TiaM contains a common Rossmann motif GxGxxG at the N-terminal for FAD- and NAD(P)H-dependent oxidoreductases, and a conserved motif WxWxIP putatively for halide-binding.⁴³ TiaM shows the highest similarity to the halogenase CrpH (39% identity) in cryptophycin biosynthesis.⁴⁴ Since there are two chlorines in **1**, TiaM probably catalyzes a dihalogenation reaction. To verify this hypothesis, the *tiaM* gene was inactivated, resulting in the mutant TCM50 (Figure S2F). HPLC-analysis of fermentation broth of TCM50 revealed the production of a major product (Figure 2G). The product was isolated and its chemical formula was determined to be C₅₂H₇₆O₁₈, lacking two chlorines, by the HRFABMS data (*m/z* 1011.4938, [M + Na]⁺; calculated, 1011.4929). Full NMR characterization (¹H, ¹³C, COSY, HSQC, and HMBC) clearly revealed the isolated compound to have the structure of **9** (Chart 2). Two additional proton signals [6.20 (d, *J* = 2.5 Hz, H-4'''), 6.26 (d, *J* = 2.5 Hz, H-6''')] were present in **9** (Tables S3 and S4, Figure S3) when comparing with **1**.² In the HMBC spectrum of **9**, these two proton signals showed strong correlations to C-2''', C-4''', C-8''', and to C-2''', C-6''', demonstrating their locations at C-6''' and C-4''', respectively. Thus, we conclude that TiaM is responsible for incorporation of two chlorines in **1**.

Genes Putatively Involved in Precursor Supply of Starter and Extender Units. Two genes in the *tia* gene cluster, *tiaC* and *tiaD*, putatively encode E1-alpha and E1-beta subunits, two components of the branched-chain alpha-keto acid dehydrogenase (BCDH) complex. BCDH complex is possibly involved in the generation of isobutyryl-CoA, propionyl-CoA, and other acyl-CoA analogues by the oxidative decarboxylation of alpha-branched-chain fatty acids derived from alpha-branched-chain amino acids.⁴⁵ However, the *tia* gene cluster lacks the other components of the BCDH complex including a dihydrolipoamide acyltransferase (E2), a dihydrolipoamide dehydrogenase (E3), and a requisite alpha-branched-chain amino acid transaminase.⁴⁶ The deduced product of *tiaL* gene displays high similarity to the propionyl-CoA carboxylase, probably catalyzing the carboxylation of propionyl-CoA to form (2*S*)-methylmalonyl-CoA.⁴⁷ The genes *tiaJ*, *tiaN*, and *tiaK* are identified to encode for hydroxybutyryl-CoA dehydrogenase, crotonyl-CoA hydratase, and crotonyl-CoA carboxylase/reductase, respectively. These enzymes were recently elucidated to be involved in the ethylmalonyl-CoA pathway.^{48,49} Especially, the crotonyl-CoA carboxylase/reductase is identified as a key enzyme and a marker for the presence of the ethylmalonyl-CoA pathway.⁴⁸ Thus, TiaJ, TiaN, and TiaK probably contribute to provide the ethylmalonyl-CoA extender unit for **1** PKS. The deduced product of *tiaE* shares high identity (61%) with NysE, a putative type II thioesterase (TE) in nystatin biosynthesis.⁵⁰ In polyketide biosynthesis, Type II TE may function as editing enzymes, likely to remove aberrant precursors.⁵¹ Thus, TiaE may be functional to promote the accuracy and efficiency of **1** PKS process.

Sugar Biosynthesis and Modifications. Tiacumicin B (**1**) bears two modified *D*-rhamnose moieties. *D*-rhamnose was biosynthesized through sequential conversion of GDP-*D*-mannose by GDP-mannose 4,6-dehydratase (Gmd) and GDP-4-keto-6-deoxymannose reductase (Rmd).⁵² Interestingly, three putative Gmds, encoded by *tiaS1*, *tiaS3*, and *tiaS4*, were identified in the *tia* gene cluster. Both TiaS3 and TiaS4 displayed high sequence identity to NysDIII (60% and 70%, respectively), a characterized Gmd involved in the mycosamine

biosynthesis of polyene antibiotic nystatin.⁵³ TiaS1 shows the highest homology (58% identity) to a putative Gmd from *Prochlorococcus marinus*.⁵⁴ However, no specific Rmds are identified. Some Gmds are found to be bifunctional and are also able to catalyze the same stereospecific reduction like Rmds;^{52,55} we suppose that at least one of TiaS1, TiaS3, and TiaS4 is functional as a Rmd. TiaS2 contains two conserved domains, methyltransf_13 [pfam08421] at N-terminus and methyltransf_14 [pfam08484] at C-terminus, characteristic for bacterial C-methyltransferases, requisite for transforming GDP-*D*-rhamnose into GDP-5-methyl-*D*-rhamnose. TiaS5 shares 39% identity with StfMIII, an *O*-methyltransferase involved in steffimycin biosynthesis.⁵⁶ TiaS5 is probably responsible for biosynthesizing 2-*O*-methyl-*D*-rhamnose. TiaG1 and TiaG2 share 50% identity to each other and both display high similarities to NysDI and AmphDI, two characterized GDP-sugar dependent GTs from nystatin and amphotericin biosynthetic gene clusters.⁵⁷ Additionally, TiaS6 is found to exhibit the closest homology to MppM, an isovaleryltransferase, in the mannopeptimycins gene cluster from *Streptomyces hygroscopicus*.⁵⁸ TiaS6 contains a conserved domain of acyltransferase_3 [pfam01757] and probably is responsible for esterifying the 7-carbon sugar with small fatty acids. Upon these bioinformatic analyses, a pathway for sugar biosynthesis and modifications is proposed, as outlined in Figure 3C.

To probe the specific functions of GTs, both *tiaG1* and *tiaG2* were inactivated via replacement with the *aac(3)IV* cassette, conferring the apramycin resistant mutants, TCM 57 and TCM 64 (Figure S2B and G), respectively. Both mutants lost the ability to produce **1** and accumulated novel products (Figure 2H,I). By fermentation of the *tiaG1*-mutant TCM57, 5 new products were isolated and 4 of them were structurally elucidated to be **11–14** (Chart 2), by HRFABMS and full NMR (¹H, ¹³C, COSY, HSQC, HMBC) spectral analyses (Tables S3 and S4, Figure S5 for **11**, Figure S6 for **12**, Figure S7 for **13**, and Figure S8 for **14**). Comparing with **1**, signals of the 7-carbon sugar residue were missing in their ¹H and ¹³C NMR spectroscopic data of compounds **11–14**; consistent with this, the C-11 was found to shift upfield about 10 ppm (Tables S3 and S4). These data confirmed that compounds **11–14** lacked the 7-carbon sugar residue at C-11 (Chart 2). The molecular formula of compound **10** was established as C₃₁H₄₈O₁₀ on the basis of HRFABMS (*m/z* 603.3110, [M + Na]⁺; calculated, 603.3145). Comparing with the compound **12**, there were no signals for aromatic moiety in **10** (Figure S4). The doublet methyl group in **12** was also absent in **10**. A unique oxygenated sp³ methylene carbon [δ_{H} 3.79 (1H, m), 3.91 (1H, m), δ_{C} 60.9 t] was found in **10**, and the C-5' in **10** was found to shift 3.2 ppm upfield (Tables S3 and S4), indicating that there was a hydroxyl group at C-6' in **10**. Therefore, the structure was deduced to be **10** (Chart 2). Subsequently, 4 new products were isolated from the *tiaG2*-mutant TCM64 and were determined to be **15–18** (Chart 2). The ¹H and ¹³C NMR spectra of **15–18** presented only one anomeric proton, suggesting the presence of a single sugar residue in these compounds. The anomeric proton showed strong HMBC correlation to C-11, and consistently, H-11 was found to have HMBC correlation to C-1'' (Tables S3 and S4, Figure S9 for **15**, Figure S10 for **16**, Figure S11 for **17**, and Figure S12 for **18**). These data unequivocally established the glycosylation at C-11 and the sugar residue at C-20 was missing in **15–18**. Taken together, our experimental facts unambiguously established that TiaG1 was the 5-*C*-methyl-*D*-rhamnosyltransferase (C-11) and TiaG2 was the 2-*O*-methyl-*D*-rhamnosyltransferase (C-20) (Figure 3C). Inactivation of *tiaS2*, a C-methyltransferase encoding gene, was also carried out to give the mutant

TCM55 (Figure S2H). The TCM55 mutant lost **1** production and accumulated 3 major products (Figure 2J). The first product (**19**) was isolated and characterized by MS (m/z 1065.3988, $[M + Na]^+$; calculated, 1065.3993) and NMR (1H , ^{13}C , COSY, HSQC, and HMBC, Figure S13). In comparison with the 1H and ^{13}C NMR spectra of **1**, two singlet methyls and the linking quaternary carbon in **1** were missing in **19**, instead, one doublet methyl [δ_H 1.13 (3H, d, $J = 6.0$ Hz, Me-6''), δ_C 18.1 (q, Me-6'')] and one methine [δ_H 3.28 (1H, dd, $J = 6.5, 9.5$ Hz, Me-5''), δ_C 71.4 (d, Me-5'')] were found in **19**, suggesting the loss of a methyl group. In the HMBC spectrum of **19**, the proton signals for the methyl doublet showed strong correlations to C-4'' and C-5'', indicating that the methyl group was located at C-5''. The large 1H , 1H coupling constant ($J = 9.5$ Hz) of H-4'' and H-5'' in C-11 sugar moiety suggested that H-4'' and H-5'' adopted axial orientations in **19**. In the NOESY spectrum of **19**, the H-5'' had correlation to axial oriented H-1'', providing further support of the axial orientation of H-5''. Thus, the compound was elucidated to have the structure of **19** (Chart 2), consistent with the prediction of TiaS2 as a sugar C-methyltransferase. The latter two products were characterized to be **12** and **13**, respectively, by comparing their retention times (18.6 min for **12** and 19.2 min for **13**) and molecular masses (m/z 819.3, $[M + Na]^+$; and m/z 425.3, $[M + Na]^+$) to standard **12** and **13**, previously isolated from TCM57 (Figure 2J,H).

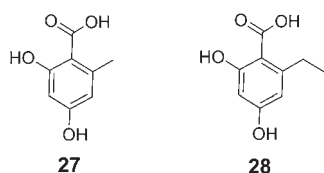
Inactivation of *tiaS6* gave the mutant TCM53 (Figure S2I), which produced two major products (Figure 2K). The first product was characterized to be **11**, deducing from its retention time (14.7 min) and molecular weight (m/z 441.3, $[M + Na]^+$) by comparison to standard **11** previously isolated from *tiaG1*-mutant TCM57 (Figure 2K,H). The latter one (**20**) was isolated and its molecular formula was established as $C_{48}H_{68}O_{16}Cl_2$ on the basis of HRFABMS (m/z 993.3831, $[M + Na]^+$; calculated, 993.3782). Comparing the 1H and ^{13}C NMR data with **1**, signals for the isobutyryl moiety were missing in **20** (Tables S3 and S4, Figure S14). Additionally, HMBC spectra of **20** showed that an ethyl group was linked to C-17, indicating no hydroxyl group at C-18 (Figure S14). Taken together, the compound was identified as **20** (Chart 2). Combining with the bioinformatic analysis (Table 1), we concluded that TiaS6 was an acyltransferase, responsible for incorporation of the isobutyryl moiety.

Genes Encoding Cytochrome P450 Hydroxylases. The *tiaP1* and *tiaP2* genes encode putative cytochrome P450 (CYP) enzymes, which belong to a large and diverse group of enzymes involved in the oxygenation of natural products. Both TiaP1 and TiaP2 contain the conserved O_2 binding motif 'LLxAGxxT' and the C-terminal heme binding site, 'FGxGx-HxCxG', typical for CYPs.⁵⁹ TiaP1 displays high similarities to LnmA and SfmO3, two CYPs involved in leinamycin and saframycin A biosynthesis,^{60,61} respectively. TiaP2 resembles a putative CYP in *Streptosporangium roseum* DSM 43021. The functions of TiaP1 and TiaP2 were investigated by *in vivo* inactivation experiments. The *tiaP1* inactivation mutant TCM 69 (Figure S2J) lost ability for **1** production (Figure 2L), and produced a new compound **21** (Chart 2; Figure S15). The compound was isolated and its molecular formula was established as $C_{52}H_{74}O_{17}Cl_2$ on the basis of HRFABMS (m/z 1063.4264, $[M + Na]^+$; calculated, 1063.4201). In comparison with 1H and ^{13}C NMR spectra of **1**, the oxygenated sp^3 methine carbon at C-18 in **1** was reduced to a methylene [δ_H 1.67 (dd, $J = 7.0, 14.0$, H-18), 1.83 (dd, $J = 7.0, 14.0$ Hz, H-18); δ_C 26.4 (t, C-18)] in **21**, and the doublet methyl in **1** was replaced by triplet methyl [δ_H 0.95 (t, $J = 7.3$ Hz, Me-19),

δ_C 10.0, Me-19] in **21**. In addition, H-19 was found to have strong HMBC correlations to C-17 (oxygenated sp^3 methine) and C-18 (methylene). These data undoubtedly supported the lack of a hydroxyl group at C-18 in **21**, confirming that TiaP1 forms the hydroxyl group at C-18. Subsequently, fermentation of the *tiaP2*-inactivation mutant TCM54 (Figure S2K) led to the production of 4 major compounds **22–25** and a minor compound **26** (Figure 2M). The compounds **22**, **23**, **25**, and **26** were isolated and characterized by HRFABMS and full NMR (1H , ^{13}C , COSY, HSQC, HMBC) spectral analyses (Tables S3 and S4; Figure S16 for **22**, Figure S17 for **23**, Figure S18 for **25**, Figure S19 for **26**). By analyzing their 1H and ^{13}C NMR data, the presence of an additional singlet methyl group and the absence of an oxygenated sp^3 methylene carbon were found in compounds **22**, **23**, and **25** (Chart 2), when comparing to compounds **15–18**, previously characterized from the *tiaG2* mutant TCM64. In HMBC spectra of these compounds, proton signals of the additional methyl group showed strong correlations to C-1 and C-3, indicating that the methyl group was located at C-20. These data confirmed that the hydroxyl group at C-20 was missing in compounds **22**, **23**, and **25**. In comparison with **25**, one triplet methyl and one methylene were missing in **26**; however, two additional doublet methyls [δ_H 0.96 (d, $J = 7.0$ Hz, Me-19), 0.97 (d, $J = 7.0$ Hz, Me-20), δ_C 19.6 (q, Me-19), 18.3 (q, Me-20)] and one methine [δ_H 2.09 (dd, $J = 7.0, 14.0$ Hz, H-18), δ_C 30.5 (d, C-18)] were found in **26**, suggesting an isopropyl group at C-17 in **26**. Consistent with this, H-19 showed strong HMBC correlations to C-17, C-18, C-20, and H-20 showed strong HMBC correlations to C-17, C-18, C-19, specifically supporting the structure of **26**. The structure of compound **24** (Chart 2) was deduced from its molecular weight via HPLC–MS analysis (m/z 641.4, $[M + Na]^+$). These new products **22–26** lack both hydroxyl groups at C-20 and C-18. Since TiaP1 was unequivocally demonstrated to be the C-18 hydroxylase, we concluded that TiaP2 specifically catalyzed the hydroxylation at C-20.

Genes Putatively Involved in Regulation, Resistance, and Transportation and Genes with Unknown Functions. The *tiaR1* gene encodes a putative LuxR class regulator [pfam00196]. Regulators of this family often appear as transcriptional activators in bacteria.⁶² Our preliminary data indicated that TiaR2 may function as a negative regulator in **1** biosynthesis (Figure 2E). Four genes, *tiaT1–T4*, are putative resistance and transporter genes found in the *tia*-gene cluster. The deduced product of *tiaT1* displays high similarity to EmrB/QacA subfamily of drug resistance transporter, belonging to the Major Facilitator Superfamily (MFS), a large and diverse group of secondary transporters. TiaT2 is homologous to Na/H antiporters, key transporters in maintaining the pH of actively metabolizing cells. TiaT3 and TiaT4 exhibit high homology to members of the ABC transporter superfamily involved in the transport of a wide variety of different compounds. Since most of **1** and its analogues are present in the fermentation broths of wild type and the mutants, TiaT1–T4 may constitute an efficient system to transport the synthesized metabolites out of the cells. However, the exact roles of TiaT1–T4 and their involvements in **1** transport remain uncertain. The *tiaI* product shows similarity to ATP-dependent superfamily I DNA and RNA helicases [COG3973]. Its function for **1** biosynthesis is not clear.

Biochemical Characterization of the Halogenase TiaM. Our *in vivo* inactivation experiment suggests that TiaM is the requisite halogenase probably catalyzing a dihalogenation reaction in **1** biosynthesis. To verify TiaM function *in vitro*, *tiaM* was

Chart 3. Chemical Structures for Orsellinic Acid (27) and Homo-orsellinic Acid (28)

amplified from NRRL 18085 genomic DNA and heterologously overexpressed in *E. coli* as an *N*-(His)₆-fused soluble protein (Figure S21). Purified recombinant TiaM exhibited a yellow color, indicating the presence of a flavin cofactor. Heat denaturation of purified TiaM released the noncovalently bound cofactor, which was identical to authentic FAD in HPLC analysis (data not shown). Since no discrete ACP was found in the *tia* gene cluster,

we suppose that TiaM probably utilize a free small molecule as a substrate. The TiaM activity was probed using orsellinic acid (27), a homo-orsellinic acid (28) mimic (Chart 3), and 9, a compound isolated from the *tiaM* mutant, as putative substrates. The reduced flavin cofactor was provided by in situ reduction of FAD by SsuE from *E. coli*.⁶³ No conversions were found for 27 (data not shown). In contrast, two new products were formed in an *in vitro* assay comprising TiaM, 9, SsuE, FAD, NADH, and NaCl (Figure 4A). Conversion rates under assayed conditions for the two products were 33% and 10% (Figure 4A), respectively. LC-MS analyses of the assay revealed that the two products had molecular weights of *m/z* 1045.5 ($[M + Na]^+$) and *m/z* 1079.4 ($[M + Na]^+$), consistent with mono- and dichlorinated 9, respectively. Subsequently, the first product (29) was isolated from a large-scale TiaM reaction and characterized by HRFABMS and full NMR (¹H, ¹³C, COSY, HSQC, HMBC) spectral analyses (Tables S3 and S4; Figure S20).

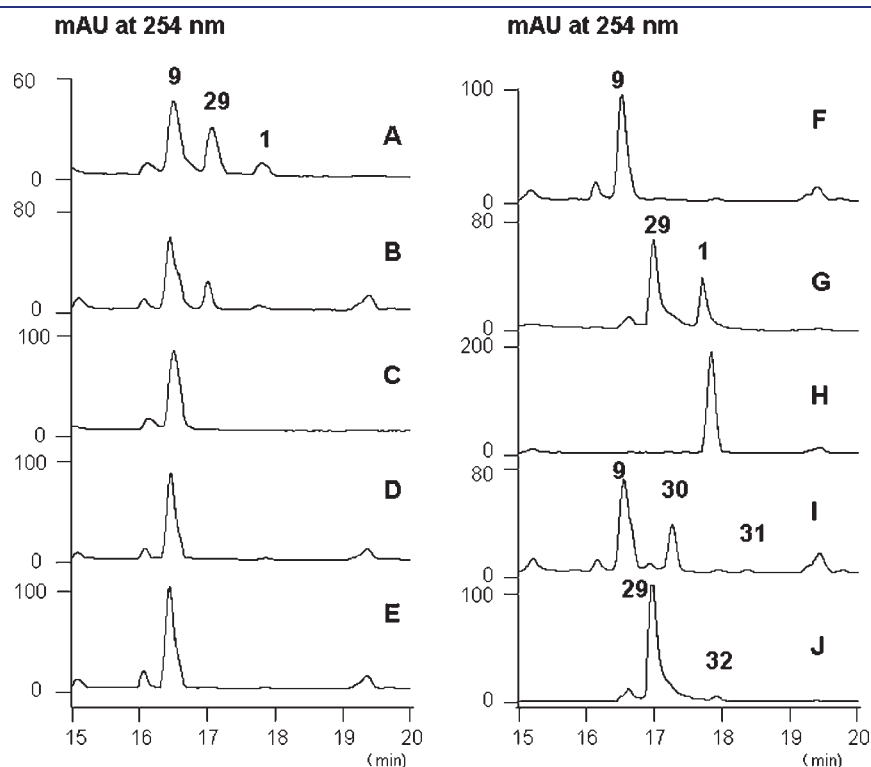
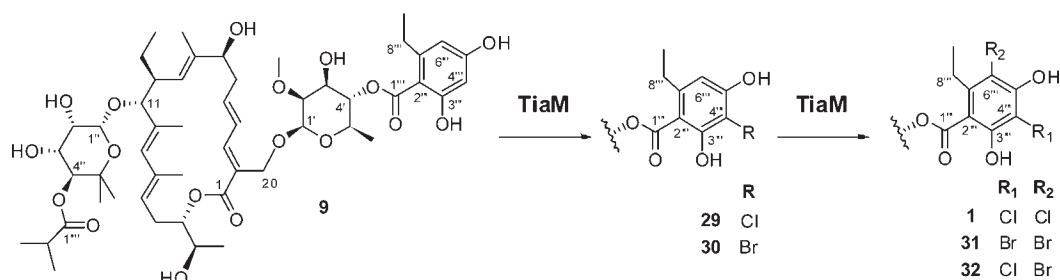
Scheme 1. A Scheme for TiaM Catalysis

Figure 4. HPLC analyses of TiaM biochemical assays. (A) A standard TiaM assay comprising 26 μ M 9, 2.9 μ M TiaM, 0.22 μ M SsuE, 0.1 mM FAD, 4 mM NADH, and 100 mM NaCl; (B) a standard assay minus SsuE; (C) an assay minus TiaM; (D) a standard assay minus FAD; (E) a standard assay minus NADH; (F) a standard assay minus NaCl; (G) a standard TiaM assay using 29 instead of 9; (H) 1 standard; (I) a standard TiaM assay using NaBr instead of NaCl; (J) a TiaM assay comprising 26 μ M 29, 2.9 μ M TiaM, 0.22 μ M SsuE, 0.1 mM FAD, 4 mM NADH, and 100 mM NaBr.

Table 2. MIC Values for **1** Analogues

$\mu\text{g/mL}$	<i>E. coli</i> ATCC	<i>S. aureus</i>	<i>B. thuringiensis</i>	<i>E. faecalis</i>
	25922	ATCC 29213		ATCC29212
1	>128	8	0.25	2
9	>128	8	2	4
10	>128	>128	>128	>128
11	>128	>128	>128	64
12	>128	16	16	>128
13	>128	>128	>128	>128
14	>128	32	8	32
15	>128	>128	>128	>128
16	>128	>128	>128	>128
17	>128	>128	>128	>128
18	>128	>128	128	>128
20	>128	128	2	32
21	>128	8	4	4
22	>128	128	128	>128
23	>128	64	64	>128
25	>128	>128	>128	>128

On the basis of HRFABMS (m/z 1045.4490, $[\text{M} + \text{Na}]^+$; calculated, 1045.4540), the molecular formula of **29** was established as $\text{C}_{52}\text{H}_{75}\text{O}_{18}\text{Cl}$. In comparison with the ^1H and ^{13}C NMR spectra of **9**, a sp^2 quaternary carbon (δ_{C} 105.8, s) was missing in **29**. The proton signals linking to the remaining sp^2 quaternary carbon showed HMBC correlations to C-2''', C-4''', and C-8''', indicating presence of H-6'''. Consistent with this, H-8''' showed HMBC correlation to C-6'''. These data undoubtedly confirmed the enzymatic product to be **29** (Scheme 1; Tables S3 and S4, Figure S20). The latter product was characterized to be **1** by comparing both retention time and molecular weight with **1** authentic standard (Figure 4H). In the absence of SsuE, TiaM retained about 60% activity, with 20% conversion to **29** and 4% conversion to **1** (Figure 4B), suggesting the presence of a presumable unknown co-purified flavin reductase.²⁵ However, absence of any component of TiaM, FAD, NADH, or Cl^- led to almost complete abolishment of the new products formation (Figure 4C–F). In the next assay, TiaM was able to transform **29** to **1** at a conversion rate of 45% (Figure 4G). These experiments demonstrated that TiaM catalyzed twice chlorinations on **9** to afford **29** and **1**, in a sequential manner, first to chlorinate at C-4''' and then at C-6''' of the **9** aromatic moiety (Scheme 1). Furthermore, we tested TiaM tolerance to different halide donors. Under assayed conditions, TiaM was capable of brominating **9** to afford 26% of **30** (m/z 1089.4, $[\text{M} + \text{Na}]^+$) and 1.4% of **31** (m/z 1169.3, $[\text{M} + \text{Na}]^+$) (Figure 4I). TiaM was also capable of converting **29** to **32** (m/z 1123.4, $[\text{M} + \text{Na}]^+$), with a very low conversion rate (1%, Figure 4J). However, F^- and I^- were not detected as halide donors for TiaM (data not shown).

Tiacumicin Derivatives and Their Antibacterial Activities. We isolated 17 new compounds from 7 mutants. To evaluate biological activities of these **1** analogues, we measured their minimum inhibitory concentration (MIC) values against 4 indicator strains, including *E. coli* ATCC 25922, *Staphylococcus aureus* ATCC 29213, *Bacillus thuringiensis*, and *Enterococcus faecalis* ATCC 29212. Our results showed that only the compounds **9**, **12**, **14**, **20**, and **21** still preserved the antimicrobial activities (Chart 2 and Table 2), implying that the 2-*O*-methyl-4-*O*-homodichloro-orsellinate- β -*D*-rhamnose moiety was critical for

antimicrobial activities. However, our results indicate that the hydroxyl group at C-18 and the two chlorines at C-4''' and C-6''' are less important for **1** bioactivity against *S. aureus* and *E. faecalis*, since compounds **21** and **9** have near equipotent activity as **1** for these two strains.

DISCUSSION

Tiacumicin B (**1**) is a halogenated macrolide belonging to polyketides, which comprise a large family of natural products with diverse biological activities and pharmacological properties. In this study, we reported the cloning and sequencing analysis of the tiacumicin B (**1**) biosynthetic gene cluster from *D. aurantiacum* NRRL 18085 and the elucidation of key biosynthetic steps by both *in vivo* genetic and *in vitro* biochemical characterizations. Isolation and structural elucidation of 18 biosynthetic intermediates from 7 key *tia*-gene inactivated mutants provided clues to dissect the biosynthetic pathway for **1**. The tiacumicinone (**13**) is biosynthesized through a complex type I PKS system comprising *tiaA1*–*tiaA4* (Figure 3A), evidenced by the complete abolishment of **1** production in *tiaA1*-inactivation mutant (Figure 2F). Interestingly, the production of **26** (Chart 2) by TCM54 indicates a promiscuous loading module capable of utilizing both propionyl- and isobutyryl-CoA as starter units in TiaA1. The substrate promiscuity of loading modules was previously demonstrated for DEBS.³⁸

By *in vivo* gene inactivation, TiaG1 and TiaG2 were characterized as the 5-*C*-methyl-*D*-rhamnosyl-transferase and the 2-*O*-methyl-*D*-rhamnosyltransferase, respectively. Interestingly, the production of the new compound **10**, bearing a mannose instead of a rhamnose moiety, by the mutant TCM57, indicates that TiaG2 can also accept a GDP-*D*-mannose as a surrogate substrate. Similarly, the production of **19** by TCM55 indicates that TiaG1 can also accept GDP-*D*-rhamnose as a non-native sugar donor. The inherent substrate flexibility is often seen for natural products GTs, making GT a versatile tool for natural product diversification.^{64,65} TiaG1 and TiaG2 are potential new members in this toolbox. However, both GT-mutants TCM57 and TCM64 can only produce monoglycosylated products, indicating that TiaG1 and TiaG2 exhibit no cross implementing functions and suggesting that TiaG1 and TiaG2 are stringent in the regiochemistry. The catalytic order of TiaG1 and TiaG2 could be arguably inferred from our results. The relative amounts of **12** and **14** produced by the *tiaG1* mutant TCM57 are quite small compared to that of **11** and **13** (Figure 2H), meaning that very little glycosylation of **11** or **13** is catalyzed by TiaG2 in the absence of TiaG1. In contrast, relative large amounts of **15**–**18** are accumulated by the *tiaG2* mutant TCM64 (Figure 2I), and no productions of **11** were detected, indicating that **11** was efficiently glycosylated by TiaG1 in the absence of TiaG2. Thus, we propose that TiaG1 catalysis probably occurs before TiaG2 (Figure 3A).

Production of **19** by TCM55 unequivocally confirmed TiaS2 as a sugar C-methyltransferase (Figure 2J and Figure 3C). C-methylation often occurs on the nucleotide sugar stage before glycosyltransfer in natural product biosynthesis, exemplified by the *in vitro* biochemical characterization of C-methyltransferases TylC3 for TDP-*L*-mycarose and EvaC for TDP-*L*-epivancosamine.^{66,67} However, timing for TiaS5-catalyzed sugar-*O*-methylation remains uncertain. In most cases, sugar *O*-methylation happens as a tailoring step;^{64,68} however, case exists for direct *O*-methylation of NDP-sugars prior to glycosyl coupling.^{69,70} Production of

20 by TCM53 reveals TiaS6 to be a sugar *O*-acyltransferase (Figure 2K and Figure 3C). However, more biochemical experiments are required to determine the timing (before or after glycosyl coupling) for TiaS6-catalyzed *O*-acylation. Interestingly, compounds 16–18 and 23–25 (Chart 2), which are different in the length of the sugar acyl-side chains, were produced by TCM64 and TCM54, suggesting that the acyltransferase TiaS6 has broad substrate specificities toward acetyl-, propionyl-, and isobutyryl-CoAs.

Our gene inactivation experiments also established that TiaP1 and TiaP2 were the C-18 and C-20-hydroxylases, respectively. Production of both 11 and 13 by TCM57 (Figure 2H and Chart 2) indicates that hydroxylation at C-20 by TiaP2 probably is an early event in 1 biosynthesis. In contrast, the lack of a hydroxyl group at C-18 in the compounds 10–18 and 21–26 (Chart 2), suggests that TiaP1 catalyzes a tailoring step that occurs later in 1 biosynthesis. Interestingly, the absence of C-18 hydroxyl group in 20, produced by *tiaS6*-inactivated mutant hints that *O*-acylation by TiaS6 probably occurs before TiaP1 catalysis. In contrast, the presence of C-18 hydroxyl group in 19 and 9, produced by TCM55 (Δ *tiaS2*) and TCM50 (Δ *tiaM*), respectively, indicates that TiaP1 preserves its activity when changing the C-11 sugar moiety and removing halogens in the aromatic ring.

The production of 9 by TCM50 suggests that TiaM was a dihalogenase. Indeed, our *in vitro* biochemical characterization confirmed that TiaM was capable of catalyzing sequential chlorinations on 9, first at the aromatic C-4''' to form 29, and then at C-6''' to furnish 1 biosynthesis. The monobrominated compound 30 (Scheme 1) was previously isolated from the wild-type producer.²⁹ These data supported that first halogenation of TiaM catalysis exhibited an exclusive regioselectivity at C-4''' of the homo-orsellinic acid moiety in 9. Previously characterized bacterial halogenases, such as PltA,²⁴ SgcC3,¹⁸ RebH,⁷¹ KtzQ, and KtzR⁷² catalyzed halogenations in early steps of natural product biosynthesis. Recently, eukaryotic halogenases ChIA²⁵ and Rdc2^{22,23} were reported for tailoring biosynthesis of DIF-1 (8) and radicicol (6), respectively. The demonstration of 9, but not 27 (Chart 3), as a TiaM substrate suggests that TiaM catalysis occurs after the TiaF-catalyzed coupling of unmodified homo-orsellinic acid with the 2-*O*-methyl-D-rhamnose residue. Thus, we concluded that TiaM functioned as a tailoring enzyme involved in 1 biosynthesis. To our best knowledge, this represents the first example of a tailoring halogenase of prokaryotic origin. Our results also hint that tailoring halogenations are probably embedded in the biosynthesis of other prokaryotic natural products, such as calicheamicin γ_1^1 (2) and avilamycin A (4),^{18,20} which harbor very similar aromatic moieties as 1 (Chart 1) and lack obvious discrete ACP encoding genes in their biosynthetic gene clusters.

Conclusively, the cloning and sequencing of the *tia* gene cluster from *D. aurantiacum* NRRL 18085 lays a foundation for further understanding of the biosynthetic logic for the antibiotic tiacumicin B of great clinical promise. The genetic manipulation of the *tia* gene cluster allows elucidation of key biosynthetic steps for 1 production, including glycosylations, hydroxylations, sugar C-methylation and *O*-acylation, and halogenations. On the basis of our data, the key transformations featuring 1 biosynthesis are outlined in Figure 3A. The accumulation of 19 biosynthetic intermediates or shunt products (9–26, Chart 2; and 29, Scheme 1), among which 17 (except 23, also known as tiacumicin A,² and 20¹⁶) were novel structures, reveals the potential of generating natural product diversity via genetic approach.

Although none of the novel compounds exhibit better antibacterial activity than 1 (Table 2), they form a small library to have potentials for further studies on their inhibitory mechanism of RNA polymerase. Finally, biochemical demonstration of TiaM as a tailoring enzyme adds knowledge to further understand nature's biohalogenation strategy.

■ ASSOCIATED CONTENT

S Supporting Information. Text for supplemental methods; Table S1, list of strains, plasmids; Table S2, list of primers; Figure S1, mapping and overlaps of selected positive cosmids; Figure S2, construction of mutants; Tables S3, S4 and Figures S3–S20, spectral data for compound characterization; Figure S21, SDS–PAGE analysis of purified proteins. This material is available free of charge via the Internet at <http://pubs.acs.org>.

■ AUTHOR INFORMATION

Corresponding Author

c Zhang2006@gmail.com; c Zhang@scsio.ac.cn

Author Contributions

[†]These authors contributed equally.

■ ACKNOWLEDGMENT

We thank Professor Meifeng Tao in Shanghai Jiao Tong University for helpful discussions. We appreciate Vanessa Zubler in Novartis Institutes for BioMedical Research (Switzerland) for graciously providing lipiarmycin A3 (tiacumicin B) as a standard. We thank Dr. U. F. Wehmeier and Prof. Dr. W. Piepersberg (Bergische University, Wuppertal, Germany) for generous gifts of the cloning vector pUCPU21. We are grateful to analytical facility of South China Sea Institute of Oceanology for recording NMR data. We want to thank anonymous reviewers for insightful comments on our manuscript. This work is supported in part by grants from the National Science Foundation for Young Scientists of China (30900035), the Funds of the Chinese Academy of Sciences for Key Topics in Innovation Engineering (KSCX2-YW-G-065, KZCX2-YW-216, KZCX2-YW-JC202, KSCX2-YW-G-073) and the National Basic Research Program of China (2010CB833805). C.Z. is a scholar of the '100 Talents Project' of Chinese Academy of Sciences (08SL111002). Y.X. and G.Z. are recipients of China Postdoctoral Science Foundation (20090460836 and 20090460837).

■ REFERENCES

- (1) Sullivan, K. M.; Spooner, L. M. *Ann. Pharmacother.* **2010**, *44*, 352–359.
- (2) Hochlowski, J. E.; Swanson, S. J.; Ranfranz, L. M.; Whittern, D. N.; Buko, A. M.; McAlpine, J. B. *J. Antibiot.* **1987**, *40*, 575–588.
- (3) Coronelli, C.; White, R. J.; Lancini, G. C.; Parenti, F. *J. Antibiot.* **1975**, *28*, 253–259.
- (4) Arnone, A.; Nasini, G.; Cavalleri, B. *J. Chem. Soc., Perkin Trans. 1* **1987**, *1*, 1353–1359.
- (5) Omura, S.; Imamura, N.; Oiwa, R.; Kuga, H.; Iwata, R.; Masuma, R.; Iwai, Y. *J. Antibiot.* **1986**, *39*, 1407–1412.
- (6) Kurabachew, M.; Lu, S. H.; Krastel, P.; Schmitt, E. K.; Suresh, B. L.; Goh, A.; Knox, J. E.; Ma, N. L.; Jiricek, J.; Beer, D.; Cynamon, M.; Petersen, F.; Dartois, V.; Keller, T.; Dick, T.; Sambandamurthy, V. K. *J. Antimicrob. Chemother.* **2008**, *62*, 713–719.

- (7) Gerber, M.; Ackermann, G. *Expert Opin. Invest. Drugs* **2008**, *17*, 547–553.
- (8) Ackermann, G.; Loffler, B.; Adler, D.; Rodloff, A. C. *Antimicrob. Agents Chemother.* **2004**, *48*, 2280–2282.
- (9) Karlowsky, J. A.; Laing, N. M.; Zhanel, G. G. *Antimicrob. Agents Chemother.* **2008**, *52*, 4163–4165.
- (10) Biedenbach, D. J.; Ross, J. E.; Putnam, S. D.; Jones, R. N. *Antimicrob. Agents Chemother.* **2010**, *54*, 2273–2275.
- (11) Wu, M. C.; Huang, C. C.; Lu, Y. C.; Fan, W. J. U.S. patent 2009/0110718 A1, Apr. 30, 2009.
- (12) Johnson, A. P. *Curr. Opin. Investig. Drugs* **2007**, *8*, 168–173.
- (13) Gualtieri, M.; Villain-Guillot, P.; Latouche, J.; Leonetti, J. P.; Bastide, L. *Antimicrob. Agents Chemother.* **2006**, *50*, 401–402.
- (14) Tupin, A.; Gualtieri, M.; Leonetti, J. P.; Brodolin, K. *EMBO J.* **2010**, *29*, 2527–2537.
- (15) Martinelli, E.; Faniuolo, L.; Tuan, G.; Gallo, G. G.; Cavalleri, B. *J. Antibiot.* **1983**, *36*, 1312–1322.
- (16) Shue, Y. K.; Hwang, C. K.; Chiu, Y. H.; Romero, A.; Babakhani, F.; Sears, P.; Okumu, F. U.S. Patent US20080269145A1, Oct. 30 2008.
- (17) Sanghvi, S.; Roach, M.; Zhou, J. F.; Mittleberg, E. M.; He, P. U.S. patent US20080176927A1, Jul. 24, 2008.
- (18) Ahlert, J.; Shepard, E.; Lomovskaya, N.; Zazopoulos, E.; Staffa, A.; Bachmann, B. O.; Huang, K.; Fonstein, L.; Czisny, A.; Whitwam, R. E.; Farnet, C. M.; Thorson, J. S. *Science* **2002**, *297*, 1173–1176.
- (19) Lin, S.; Van Lanen, S. G.; Shen, B. *J. Am. Chem. Soc.* **2007**, *129*, 12432–12438.
- (20) Weitnauer, G.; Muhlenweg, A.; Trefzer, A.; Hoffmeister, D.; Sussmuth, R. D.; Jung, G.; Welzel, K.; Vente, A.; Girreser, U.; Bechthold, A. *Chem. Biol.* **2001**, *8*, 569–581.
- (21) Jia, X. Y.; Tian, Z. H.; Shao, L.; Qu, X. D.; Zhao, Q. F.; Tang, J.; Tang, G. L.; Liu, W. *Chem. Biol.* **2006**, *13*, 575–585.
- (22) Zeng, J.; Zhan, J. *ChemBioChem* **2010**, *11*, 2119–2123.
- (23) Zhou, H.; Qiao, K.; Gao, Z.; Vederas, J. C.; Tang, Y. *J. Biol. Chem.* **2010**, *10.1074/jbc.M110.183574*.
- (24) Dorrestein, P. C.; Yeh, E.; Garneau-Tsodikova, S.; Kelleher, N. L.; Walsh, C. T. *Proc. Natl. Acad. Sci. U.S.A.* **2005**, *102*, 13843–13848.
- (25) Neumann, C. S.; Walsh, C. T.; Kay, R. R. *Proc. Natl. Acad. Sci. U.S.A.* **2010**, *107*, 5798–5803.
- (26) Vaillancourt, F. H.; Yeh, E.; Vosburg, D. A.; Garneau-Tsodikova, S.; Walsh, C. T. *Chem. Rev.* **2006**, *106*, 3364–3378.
- (27) Neumann, C. S.; Fujimori, D. G.; Walsh, C. T. *Chem. Biol.* **2008**, *15*, 99–109.
- (28) Blasiak, L. C.; Drennan, C. L. *Acc. Chem. Res.* **2009**, *42*, 147–155.
- (29) Hochlowski, J. E.; Jackson, M.; Rasmussen, R. R.; Buko, A. M.; Clement, J. J.; Whittern, D. N.; McAlpine, J. B. *J. Antibiot.* **1997**, *50*, 201–205.
- (30) Sambrook, J.; Fritsch, E. F.; Maniatis, T. *Molecular Cloning: A Laboratory Manual*; 2nd ed.; Cold Spring Harbor Laboratory Press: Cold Spring Harbor, N.Y., 1989.
- (31) Kieser, T.; Bibb, M. J.; Buttner, M. J.; Chater, K. F.; Hopwood, D. A. *Practical Streptomyces Genetics*; John Innes Foundation: Norwich, 2000.
- (32) Hornung, A.; Bertazzo, M.; Dziarnowski, A.; Schneider, K.; Welzel, K.; Wohlert, S. E.; Holzenkampfer, M.; Nicholson, G. J.; Bechthold, A.; Sussmuth, R. D.; Vente, A.; Pelzer, S. *ChemBioChem* **2007**, *8*, 757–766.
- (33) Gust, B.; Challis, G. L.; Fowler, K.; Kieser, T.; Chater, K. F. *Proc. Natl. Acad. Sci. U.S.A.* **2003**, *100*, 1541–1546.
- (34) Gust, B.; Chandra, G.; Jakimowicz, D.; Yuqing, T.; Bruton, C. J.; Chater, K. F. *Adv. Appl. Microbiol.* **2004**, *54*, 107–128.
- (35) Xiao, Y.; Li, S.; Ma, L.; Zhang, G.; Ju, J.; Zhang, C. *Acta Microbiol. Sin.* **2010**, *50*, 1014–1022.
- (36) Shue, Y. K.; Du, C. J.; Chiou, M. H.; Wu, M. C.; Chen, Y. T.; Okumu, F. W.; Duffield, J. J. Patent WO/2004/014295, Feb. 19, 2004.
- (37) Pereda, A.; Summers, R. G.; Stassi, D. L.; Ruan, X.; Katz, L. *Microbiology* **1998**, *144* (Pt. 2), 543–553.
- (38) Lau, J.; Cane, D. E.; Khosla, C. *Biochemistry* **2000**, *39*, 10514–10520.
- (39) Reeves, C. D.; Murli, S.; Ashley, G. W.; Piagentini, M.; Hutchinson, C. R.; McDaniel, R. *Biochemistry* **2001**, *40*, 15464–15470.
- (40) Shao, L.; Qu, X. D.; Jia, X. Y.; Zhao, Q. F.; Tian, Z. H.; Wang, M.; Tang, G. L.; Liu, W. *Biochem. Biophys. Res. Commun.* **2006**, *345*, 133–139.
- (41) Bevitt, D. J.; Cortes, J.; Haydock, S. F.; Leadlay, P. F. *Eur. J. Biochem.* **1992**, *204*, 39–49.
- (42) He, Q. L.; Jia, X. Y.; Tang, M. C.; Tian, Z. H.; Tang, G. L.; Liu, W. *ChemBioChem* **2009**, *10*, 813–819.
- (43) van Pee, K. H.; Patallo, E. P. *Appl. Microbiol. Biotechnol.* **2006**, *70*, 631–641.
- (44) Magarvey, N. A.; Beck, Z. Q.; Golakoti, T.; Ding, Y.; Huber, U.; Hemscheidt, T. K.; Abelson, D.; Moore, R. E.; Sherman, D. H. *ACS Chem. Biol.* **2006**, *1*, 766–779.
- (45) Denoya, C. D.; Fedechko, R. W.; Hafner, E. W.; McArthur, H. A.; Morgenstern, M. R.; Skinner, D. D.; Stutzman-Engwall, K.; Wax, R. G.; Wernau, W. C. *J. Bacteriol.* **1995**, *177*, 3504–3511.
- (46) Perham, R. N. *Biochemistry* **1991**, *30*, 8501–8512.
- (47) Chan, Y. A.; Podevels, A. M.; Kevany, B. M.; Thomas, M. G. *Nat. Prod. Rep.* **2009**, *26*, 90–114.
- (48) Erb, T. J.; Berg, I. A.; Brecht, V.; Muller, M.; Fuchs, G.; Alber, B. E. *Proc. Natl. Acad. Sci. U.S.A.* **2007**, *104*, 10631–10636.
- (49) Eustaquio, A. S.; McGlinchey, R. P.; Liu, Y.; Hazzard, C.; Beer, L. L.; Florova, G.; Alhamadsheh, M. M.; Lechner, A.; Kale, A. J.; Kobayashi, Y.; Reynolds, K. A.; Moore, B. S. *Proc. Natl. Acad. Sci. U.S.A.* **2009**, *106*, 12295–12300.
- (50) Brautaset, T.; Sekurova, O. N.; Sletta, H.; Ellingsen, T. E.; Strom, A. R.; Valla, S.; Zotchev, S. B. *Chem. Biol.* **2000**, *7*, 395–403.
- (51) Koglin, A.; Lohr, F.; Bernhard, F.; Rogov, V. V.; Frueh, D. P.; Strieter, E. R.; Mofid, M. R.; Guntert, P.; Wagner, G.; Walsh, C. T.; Marahiel, M. A.; Dotsch, V. *Nature* **2008**, *454*, 907–911.
- (52) Kneidinger, B.; Graninger, M.; Adam, G.; Puchberger, M.; Kosma, P.; Zayni, S.; Messner, P. *J. Biol. Chem.* **2001**, *276*, 5577–5583.
- (53) Nedal, A.; Sletta, H.; Brautaset, T.; Borgos, S. E.; Sekurova, O. N.; Ellingsen, T. E.; Zotchev, S. B. *Appl. Environ. Microbiol.* **2007**, *73*, 7400–7407.
- (54) Kettler, G. C.; Martiny, A. C.; Huang, K.; Zucker, J.; Coleman, M. L.; Rodrigue, S.; Chen, F.; Lapidus, A.; Ferriera, S.; Johnson, J.; Steglich, C.; Church, G. M.; Richardson, P.; Chisholm, S. W. *PLoS Genet.* **2007**, *3*, e231.
- (55) King, J. D.; Poon, K. K.; Webb, N. A.; Anderson, E. M.; McNally, D. J.; Brisson, J. R.; Messner, P.; Garavito, R. M.; Lam, J. S. *FEBS J.* **2009**, *276*, 2686–2700.
- (56) Gullon, S.; Olano, C.; Abdelfattah, M. S.; Brana, A. F.; Rohr, J.; Mendez, C.; Salas, J. A. *Appl. Environ. Microbiol.* **2006**, *72*, 4172–4183.
- (57) Zhang, C.; Moretti, R.; Jiang, J.; Thorson, J. S. *ChemBioChem* **2008**, *9*, 2506–2514.
- (58) Magarvey, N. A.; Haltli, B.; He, M.; Greenstein, M.; Hucul, J. A. *Antimicrob. Agents Chemother.* **2006**, *50*, 2167–2177.
- (59) Olano, C.; Gomez, C.; Perez, M.; Palomino, M.; Pineda-Lucena, A.; Carbajo, R. J.; Brana, A. F.; Mendez, C.; Salas, J. A. *Chem. Biol.* **2009**, *16*, 1031–1044.
- (60) Li, L.; Deng, W.; Song, J.; Ding, W.; Zhao, Q. F.; Peng, C.; Song, W. W.; Tang, G. L.; Liu, W. *J. Bacteriol.* **2008**, *190*, 251–263.
- (61) Cheng, Y. Q.; Tang, G. L.; Shen, B. *J. Bacteriol.* **2002**, *184*, 7013–7024.
- (62) Nasser, W.; Reverchon, S. *Anal. Bioanal. Chem.* **2007**, *387*, 381–390.
- (63) Eichhorn, E.; van der Ploeg, J. R.; Leisinger, T. *J. Biol. Chem.* **1999**, *274*, 26639–26646.
- (64) Thibodeaux, C. J.; Melancon, C. E.; Liu, H. W. *Angew. Chem., Int. Ed. Engl.* **2008**, *47*, 9814–9859.
- (65) Zhang, C.; Griffith, B. R.; Fu, Q.; Albermann, C.; Fu, X.; Lee, I. K.; Li, L.; Thorson, J. S. *Science* **2006**, *313*, 1291–1294.
- (66) Chen, H.; Zhao, Z.; Hallis, T. M.; Guo, Z.; Liu, H.-w. *Angew. Chem., Int. Ed. Engl.* **2001**, *40*, 607–610.

(67) Chen, H.; Thomas, M. G.; Hubbard, B. K.; Losey, H. C.; Walsh, C. T.; Burkart, M. D. *Proc. Natl. Acad. Sci. U.S.A.* **2000**, *97*, 11942–11947.

(68) Zhang, C.; Albermann, C.; Fu, X.; Peters, N. R.; Chisholm, J. D.; Zhang, G.; Gilbert, E. J.; Wang, P. G.; Van Vranken, D. L.; Thorson, J. S. *ChemBioChem* **2006**, *7*, 795–804.

(69) Schulman, M. D.; Acton, S. L.; Valentino, D. L.; Arison, B. H. *J. Biol. Chem.* **1990**, *265*, 16965–16970.

(70) Zhang, C.; Albermann, C.; Fu, X.; Thorson, J. S. *J. Am. Chem. Soc.* **2006**, *128*, 16420–16421.

(71) Yeh, E.; Garneau, S.; Walsh, C. T. *Proc. Natl. Acad. Sci. U.S.A.* **2005**, *102*, 3960–3965.

(72) Heemstra, J. R., Jr.; Walsh, C. T. *J. Am. Chem. Soc.* **2008**, *130*, 14024–14025.